Scientia Iranica B (2020) 27(3), 1197–1205

Sharif University of Technology
Scientia Iranica
Transactions B: Mechanical Engineering
http://scientiairanica.sharif.edu

Experimental investigation into the effects of Mach number and boundary-layer bleed on flow stability of a supersonic air intake

J. Sepahi-Younsi[a,*], M.R. Soltani[b], M. Abedi[b], and M. Masdari[c]

a. *Mechanical Engineering Department, Faculty of Engineering, Ferdowsi University of Mashhad, Mashhad, P.O. Box 9177948974, Iran.*
b. *Department of Aerospace Engineering, Sharif University of Technology, Tehran, Iran.*
c. *Faculty of New Science and Technologies, University of Tehran, Tehran, Iran.*

Received 6 February 2017; received in revised form 11 August 2018; accepted 5 January 2019

KEYWORDS
Supersonic air intake;
Buzz phenomenon;
Mach number;
Boundary layer bleed;
Oscillation frequency;
Bleed exit area.

Abstract. A series of experiments were conducted to study impacts of the free-stream Mach number, back pressure, and bleed on the stability of a supersonic intake. The flow stability is related to the buzz phenomenon, i.e. the oscillation of all shock waves of the intake, which may also occur when the intake mass flow rate is decreasing. In this study, the intake was axisymmetric with Mach number of 2.0. The results showed that stability margin of the intake decreased when the freestream Mach number increased for both bleed-off and bleed-on cases. In the configuration without bleed, the frequency of buzz oscillation increased when the freestream Mach number decreased or when back pressure increased. By applying bleed and, consequently, preventing separation of the flow, the intake became more stable and the shocks oscillated with a smaller amplitude during the buzz phenomenon. Also, when the bleed was applied, the buzz triggering mechanism varied from the Dailey criterion to the Ferri one, which considerably changed stability characteristics of the intake.

1. Introduction

Air intake is the main component of an aerial engine. For an efficient combustion process, the intake should deliver the required amount of flow with the maximum possible uniformity and total pressure to the engine [1]. However, back pressure fluctuations may result in shock oscillation ahead of the intake, which is named buzz [2,3]. This phenomenon can lead to vehicle thrust reduction and even combustion extinction [4].

Buzz oscillations are self-excited and self-sustainable fluctuations and occur because of flow separation [5]. Buzz initiation can be described by two main criteria; one is called the Ferri criterion [6], which states that the buzz is initiated when the vortex sheet originating from the intersection point of oblique and normal shocks impinges upon the lower surface of the cowl, and the other is called the Dailey [7] criterion, stating that flow separation over the compression surface downstream of the interaction of the shock wave and boundary layer causes the flow to be choked at the intake throat and finally, triggers the buzz oscillations [3].

Little and big buzz was first observed and in-

*. *Corresponding author.*
E-mail addresses: jsepahi@um.ac.ir (J. Sepahi-Younsi); msoltani@sharif.edu (M.R. Soltani); abedi.aerospace@gmail.com (M. Abedi); m.masdari@ut.ac.ir (M. Masdari)

doi: 10.24200/sci.2019.21683

troduced by Fisher et al. [8]. When the intake mass flow rate decreases due to the back pressure increment, small-amplitude oscillations will be first observed that are due to the Ferri criterion and called little buzz. However, as the mass flow rate further decreases, large-amplitude oscillations, namely big buzz, will be generated that are thought to be because of the Dailey criterion. Fisher et al. claimed that the frequencies of little and big buzz were similar. However, later investigations [9] showed that this could be considered as the general case.

Newsome [10] attempted to find a relation between the buzz phenomenon and the acoustic nature of the intake duct. He proposed that the fundamental frequency of the acoustic resonant was approximately equal to the buzz frequency [3].

Other researchers further investigated analytical models for predicting the buzz characteristics [11–17]. However, they were unable to develop a reliable analytical method to predict the buzz characteristics. Therefore, numerical [10,18–32] or experimental [3,9,14,24,26,28,33–47,48,49] methods are usually used to study the buzz phenomenon [3].

Various methods such as variable geometry [1], insertion of a constant area duct inside the intake [6], inserting vortex generator [50–51], applying the boundary layer suction [2,6,9,31,34,38–43,50–54], and boundary layer blowing [50] have been proposed for delaying the buzz onset. However, among all of these schemes, boundary layer suction is often used due to its simplicity and high efficiency.

Furthermore, in most studies, the bleed is in the throat to get the best performance improvement of the intake. However, according to the Dailey criterion mentioned earlier, flow separation over the compression surface is the main mechanism that triggers the buzz phenomenon.

In this study, the bleed was applied upstream of the throat and its effects on the intake stability characteristics were experimentally investigated. In addition, effects of the freestream Mach number and exit area of the bleed duct on the buzz phenomenon for the current mixed compression supersonic air intake were inquired. The intake was an axisymmetric one designed for the freestream Mach number of 2.0. However, wind tunnel tests were conducted for freestream Mach numbers of 1.8, 2.0, and 2.2 at the angle of attack of zero degree. For every freestream Mach number, several back pressures were imposed at the intake outlet to further study both the design and off-design operating conditions.

2. Experimental equipment

The intake model used in these experiments is shown in Figure 1(a). The details of the model, wind tunnel, and pressure measurements can be found in [48,55]. The spike tip had a base cone without the bleed slot and might be substituted with another cone equipped with the bleed slot (Figure 1(b)). As seen in Figure 1(c), the bleed slot was normal to the ramp surface located at $x/d = 0.3$ (d is the maximum model diameter). The ratio of the bleed entrance area to the area of the intake entrance was 10.5%.

To further study effects of the bleed exit area, two exit diffusers with different exit areas could be attached to the end of the bleed duct as shown in Figure 2(a). The area of the bleed duct A_r, shown in Figure 2(a), was about three percent of the intake entrance area. Bleed exit diffusers had exit areas of $A_e = 4A_r$ and $A_e = 2A_r$. These values were chosen arbitrarily to study variations of the intake stability characteristics with respect to the bleed exit area. The maximum value of the bleed mass flow rate obtained using this bleed system was about 2% of the intake mass flow rate.

Shadowgraph flow visualization system was used for all test cases. Mirrors and spotlight source were arranged in the Z-type configuration and an accurate table with two degrees of freedom was used to locate the knife edge (razor blade in this case) at the focal point of the receiving part. A charge-coupled device camera, namely AOS X-PRI, with recording speed of up to 1000 frames per second (fps) and image dimensions of 800×600 pixels was used for taking the pictures. This speed was enough for most test cases investigated in this study. The performance parameters used in this study include total pressure recovery, η, and mass flow ratio, ε. The definitions of these parameters along with Exit Blockage Ratio (EBR) are in [55].

The bleed mass flow ratio, ε_b, is defined as the ratio of the bleed mass flow rate to the intake mass flow rate:

$$\varepsilon_b = \frac{\dot{m}_b}{\dot{m}_i}. \tag{1}$$

The bleed mass flow rate is calculated from the data collected by a static pressure tap and a total pressure probe installed at the exit of the bleed duct [56]:

$$\dot{m}_b = \frac{P_{t,b}}{\sqrt{RT_{t,b}}} M_b A_r \sqrt{\gamma} \left(1 + \frac{\gamma - 1}{2} M_b^2\right)^{-\left[\frac{\gamma+1}{2(\gamma-1)}\right]}, \tag{2}$$

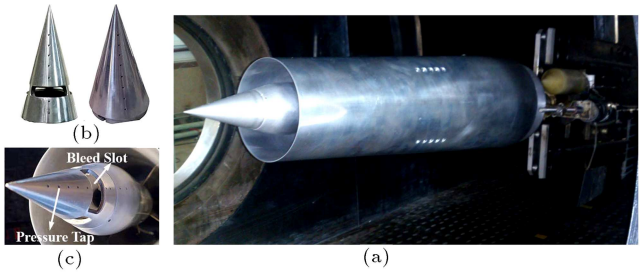

Figure 1. (a) Present intake installed in the wind tunnel. (b) Two tip cones. (c) Pressure taps and bleed slot.

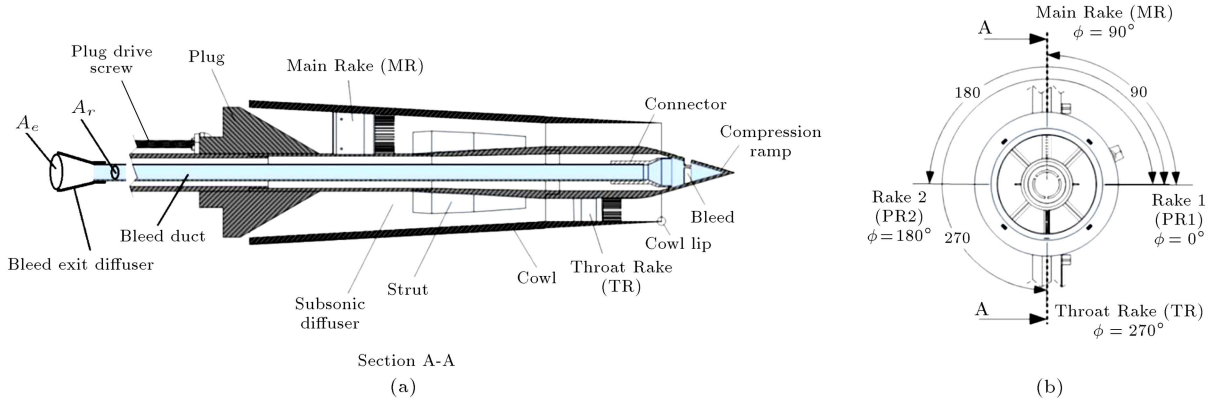

Figure 2. Schematic of the intake model and its instruments [55].

where the total temperature inside the bleed duct, $T_{t,b}$, is equal to its freestream value; Mach number at the exit of the bleed duct, M_b, is calculated by the static and total pressure sensors; and A_r is the area of the bleed duct as shown in Figure 2(a).

To study the effects of Mach number and bleed on the flow stability of the intake, stability margin, SM, is defined as:

$$SM = \frac{EBR_{Buzz\ Triggering} - EBR_{Critical\ Condition}}{EBR_{Critical\ Condition}} \times 100. \quad (3)$$

As seen, a high value of SM means that the buzz starts with a long delay and the intake is more stable.

3. Results and discussions

3.1. Effects of boundary layer suction and freestream Mach number

All the results for the configuration with bleed in this section are for the larger bleed exit area, i.e. $A_e = 4Ar$, and the effects of the smaller exit area will be studied in the next section. Performance curves of the intake with and without the boundary-layer bleed for freestream Mach numbers of 1.8, 2.0, and 2.2 are illustrated in Figure 3. Each point in this figure is for a specific value of EBR. Therefore, every curve has eight points; the farthest right point, i.e. maximum ε, is for the EBR of 55% and the first point, i.e. the lowest ε, is for the EBR of 80%. As seen from this figure, the critical operating condition is obtained at about EBR = 62.5% for both cases with and without the bleed. Therefore, SM was computed using this value. Buzz initiation was further clarified by the shadowgraph pictures and spectra of the pressure signals of high-frequency transducers [57]. Spectra of the signals were computed using Fast Fourier Transform (FFT) algorithm. According to Figure 3, when the bleed is applied, significant improvement in intake performance and increase in intake stability margin are obtained for each freestream Mach number. For $M_\infty = 1.8$, the intake becomes completely stable for all EBRs examined in this research with bleed in configuration. The values of SM are presented in Table 1. As seen in this table, SM in the no-bleed condition is reduced when the freestream Mach number increases. In fact, shock waves become stronger when the freestream Mach number increases. This results in a larger flow separation behind the shock waves. Strong flow separation favors initiation of the buzz oscillations and consequently, buzz starts at a lower EBR; as a result, SM decreases.

The dominant frequencies of buzz oscillations and the corresponding mean values of ε for various

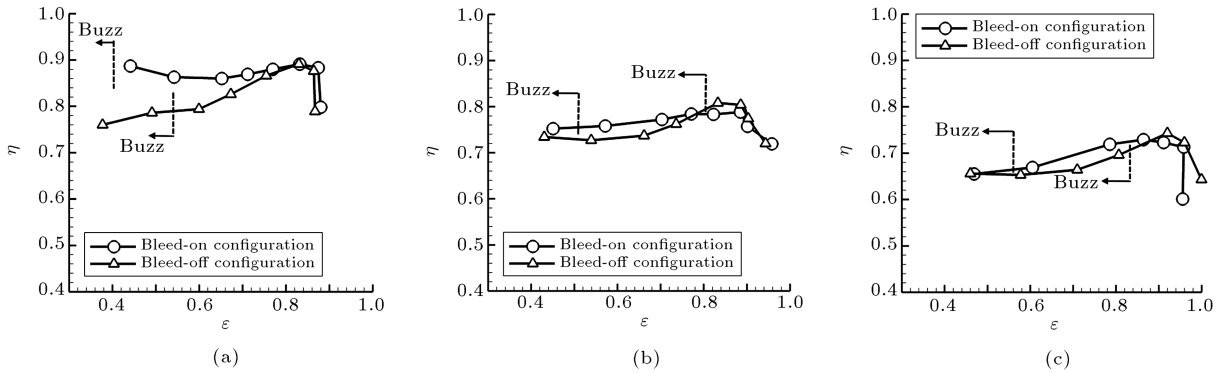

Figure 3. Performance curves of the intake with and without bleed: (a) $M_\infty = 1.8$, (b) $M_\infty = 2.0$, and (c) $M_\infty = 2.2$.

Table 1. Stability margin of the intake.

Configuration	SM (%)		
	$M_\infty = 1.8$	$M_\infty = 2.0$	$M_\infty = 2.2$
Without bleed	20.0	8.0	8.0
With bleed	> 28.0	28.0	28.0

EBRs for the no-bleed case are presented in Table 2. Buzz frequencies are obtained from the spectra of pressure signals of high-frequency transducers as shown in Figure 4 for various EBRs at a freestream Mach number of 2.0 with sensor S1 located at the tip of the spike. The sensor is shown on the top right side of Figure 4 for clarity. The values of these frequencies were validated using the shadowgraph pictures given the time step between two consecutive pictures (from the frame rate of the shadowgraph camera) by counting the number of pictures for a complete buzz cycle. As seen in Table 2, for $M_\infty = 1.8$, two different frequencies are obtained. Smaller values can be neglected due to their small amplitudes.

The shadowgraph data for all cases presented in Table 2 reveal that oscillating shock waves move forward and reach the spike tip during the buzz cycles. Thus, both frequency and amplitude of these oscillations are large and they cannot be categorized under either little or big buzz phenomenon.

Variation of buzz frequency with mass flow ratio is depicted in Figure 5. It is seen that while buzz frequency varies with the mass flow ratio, its variation with Mach number is not significant. This finding is compatible with the results of [46]. According to the figure, as the intake mass flow ratio decreases, buzz frequency increases. However, when the freestream Mach number increases, buzz frequency decreases.

Table 2. Dominant frequency of buzz oscillations and the mean value of ε for the no-bleed case.

EBR (%)	ε	Freq. (Hz)
	$M_\infty = 1.8$	
75.0	0.498	118, 485
80.0	0.383	151, 493
	$M_\infty = 2.0$	
67.5	0.744	91
70.0	0.669	96
75.0	0.546	113
80.0	0.435	127
	$M_\infty = 2.2$	
67.5	0.813	80
70.0	0.716	84
75.0	0.583	104
80.0	0.464	120

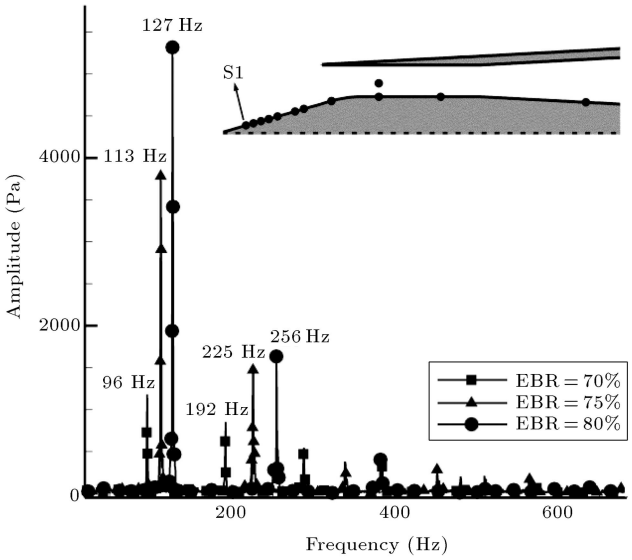

Figure 4. The spectrum of pressure signal of sensor S1 for $M_\infty = 2.0$.

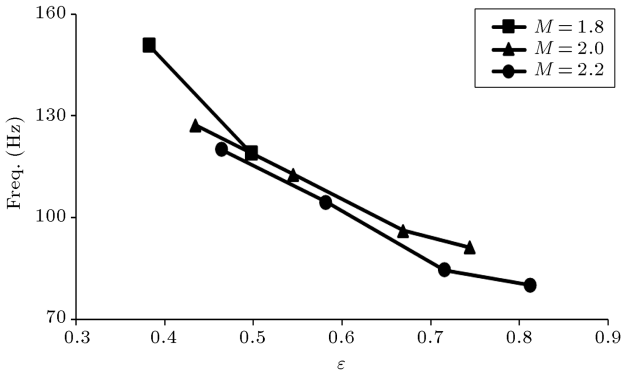

Figure 5. Variation of buzz frequency with mass flow ratio in the bleed-off configuration.

Choking the flow over the plug at the end of the model and filling the model with high-pressure air are determinative features of the buzz cycle [5]. When EBR increases and consequently, ε decreases, these features appear sooner. Therefore, the period of the buzz cycle decreases, leading to increase in the frequency of buzz oscillations. In addition, as the freestream Mach number increases, shocks reach a position closer to the throat section. Hence, buzz frequency decreases. At this position, the shocks are weaker and consequently, the separation region behind them is reduced. This, in turn, postpones the establishment of the required conditions for buzz triggering according to the Dailey criterion.

High frequencies for $M_\infty = 1.8$ as compared with other examined freestream Mach numbers are due to the starting characteristics of the current intake. As

mentioned before, the first starting Mach number of the intake is about 2.0. As a result, for $M_\infty = 1.8$, a normal shock stands near the intake entrance and the mass flow rate passing through the intake decreases due to flow spillage around the cowl lip. As shown in Figure 6, flow spillage causes the intake to be discharged from the high-pressure air in a short time and, as a result, the period of the buzz cycles is considerably reduced.

Analysis of the buzz oscillations for the no-bleed case shows that the buzz occurs according to the Dailey criterion in this intake [57]. Therefore, it is anticipated that when the boundary layer suction is applied over the spike surface, it prevents flow separation, which affects the stability characteristics of the intake. As seen in Figure 3 and Table 1, when the bleed is applied, stability margin of the intake significantly increases. For EBRs tested in this investigation, at $M_\infty = 1.8$, the buzz is completely eliminated while at $M_\infty = 2.0$ and 2.2, it starts with EBR > 75% for the configuration equipped with bleed.

The dominant frequencies of buzz oscillations and the corresponding mean values of ε are presented for the configuration equipped with bleed in Table 3. According to this table, the buzz frequency at EBR = 80% is much larger than that in the configuration without bleed. In addition, in contrast with the no-bleed case, when the freestream Mach number increases, buzz frequency also increases.

The shadowgraph pictures of the last stable EBR, i.e. EBR = 75%, for freestream Mach numbers of 2.0 and 2.2 are shown in Figure 7. As seen in this figure, all the three shocks, namely conical, barrier, and normal, intersect at such a point and the resulting vortex sheet may impinge upon the lower surface of the cowl (Ferri criterion). In addition, investigation into the shadowgraph pictures for cases with buzz reveals that in contrast with the bleed-off configuration, shocks oscillate in a limited domain outside the intake in the bleed-on configuration case. As a result, initiation and characteristics of oscillations are moved from Dailey criterion to Ferri criterion when the boundary layer suction is applied and this is the reason for differing frequency values as well as their trends from those in the bleed-off configuration.

Table 3. Dominant frequency of buzz oscillations and the mean value of ε for the bleed-on configuration.

EBR (%)	ε	Freq. (Hz)
	$M_\infty = 1.8$	
80.0	0.441	Stable
	$M_\infty = 2.0$	
75.0	0.572	Stable
80.0	0.451	898
	$M_\infty = 2.2$	
75.0	0.605	Stable
80.0	0.468	942

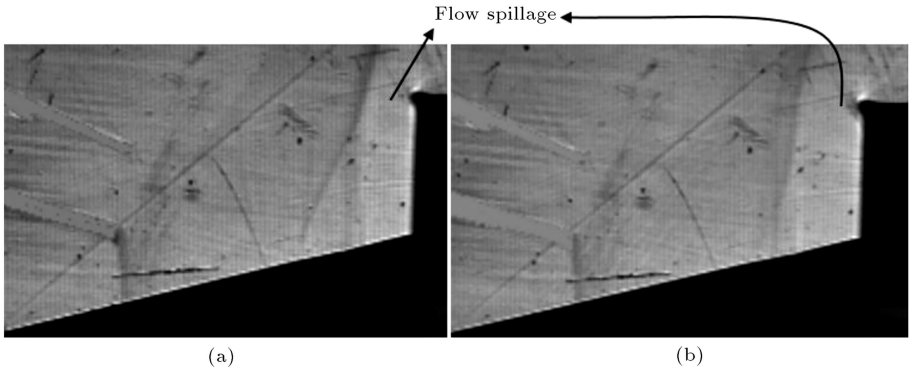

Figure 6. Shadowgraph pictures for the no-bleed case at $M_\infty = 1.8$ and at the lowest downstream position of the oscillating shock wave: (a) EBR = 75.0% and (b) EBR = 80.0%.

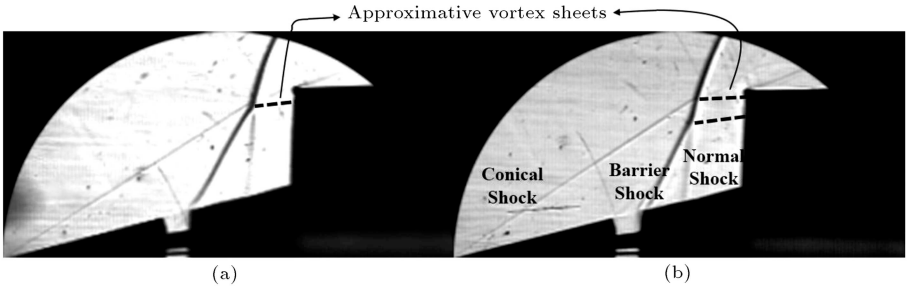

Figure 7. Shadowgraph pictures for the bleed-on case at EBR = 75.0%: (a) $M_\infty = 2.2$ and (b) $M_\infty = 2.0$.

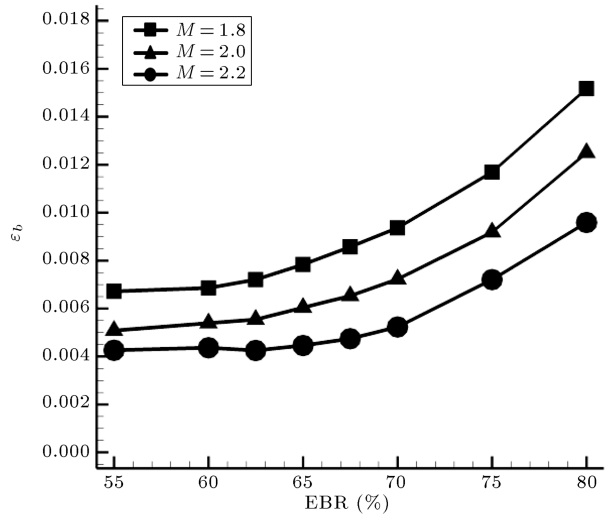

Figure 8. Variation of the bleed mass flow ratio for different EBRs.

Variations of the bleed mass flow ratio for each freestream Mach number are shown in Figure 8. According to this figure, as the freestream Mach number increases, εb for a constant value of EBR decreases. This reduction is due to the high tangential velocity near the wall for higher Mach numbers that causes less mass flow rate to enter the bleed duct. At the subcritical operating condition, i.e. larger EBRs, the value of EBR further increases. This increment in εb is because of the boundary layer thickening upstream of the bleed entrance. Finally, when the bleed is applied with a mass flow rate less than about 1.6% of the intake mass flow rate, the intake becomes more stable and the oscillation amplitude decreases.

3.2. Effects of the bleed duct exit area

As mentioned before, the previous results were for the larger bleed exit area, i.e. $A_e = 4A_r$. However, to further study the effects of the bleed exit area, tests were conducted with the smaller exit area of $A_e = 2A_r$ and the results are presented in this section. Performance curves of the intake for both bleed exit areas at freestream Mach numbers of 1.8, 2.0, and 2.2 are shown in Figure 9. As seen in this figure, the exit area of the bleed duct has negligible effects on the intake performance. However, the smaller exit area is seen to produce a higher pressure recovery, η, at freestream Mach numbers of 2.0 and 2.2. In addition, it is seen that the buzz onset and consequently, the stability margin of the intake are independent of the exit area. Hence, the values of SM for both exit areas are higher than 28.0%, 28.0%, and 28.0% at $M_\infty = 1.8$, 2.0, and 2.2, respectively.

Table 4. Buzz frequencies for two bleed exit areas.

Bleed Exit area	Freq. (Hz)	
	$M_\infty = 2.0$, EBR = 80%	$M_\infty = 2.2$, EBR = 80%
$A_e = 4A_r$	898	942
$A_e = 2A_r$	899	940

The frequencies of oscillations for both bleed exit areas at EBRs that are associated with the buzz phenomenon are presented in Table 4. As seen, the bleed exit area does not have effects on the buzz frequency. Furthermore, in Figure 10, it is seen that the exit area does not change the bleed mass flow ratio except for the freestream Mach number of $M_\infty = 2.2$. As a result, it can be concluded that the exit area of the bleed duct does not alter the stability characteristics of the intake and it has negligible effects on the intake performance.

4. Conclusions

The stability characteristics of a supersonic mixed compression axisymmetric air intake were experimentally investigated. The intake design Mach number was 2.0. However, tests were conducted for freestream Mach numbers of 1.8, 2.0, and 2.2 at zero-degree angle of attack. Several back pressures were imposed on the end of the intake for each freestream Mach number and effects of the boundary layer suction as well as

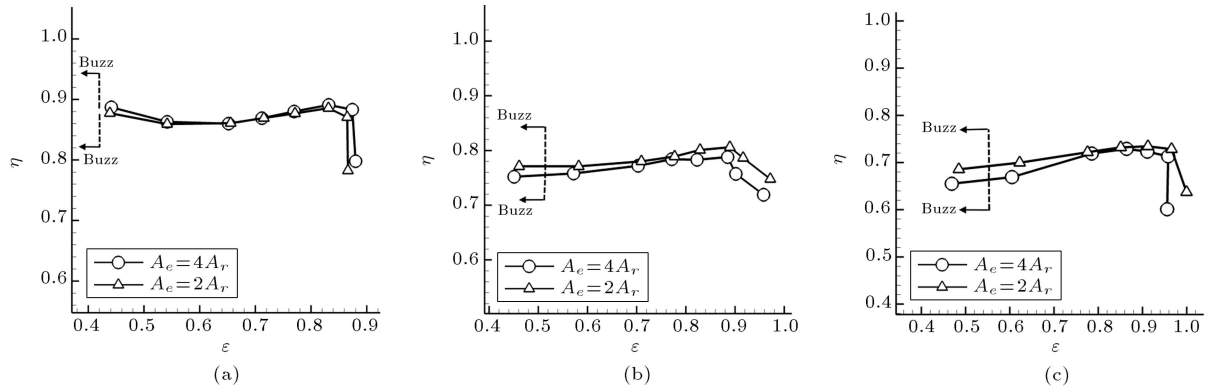

Figure 9. Performance curves of the intake for two bleed duct exit areas: (a) $M_\infty = 1.8$, (b) $M_\infty = 2.0$, and (c) $M_\infty = 2.2$.

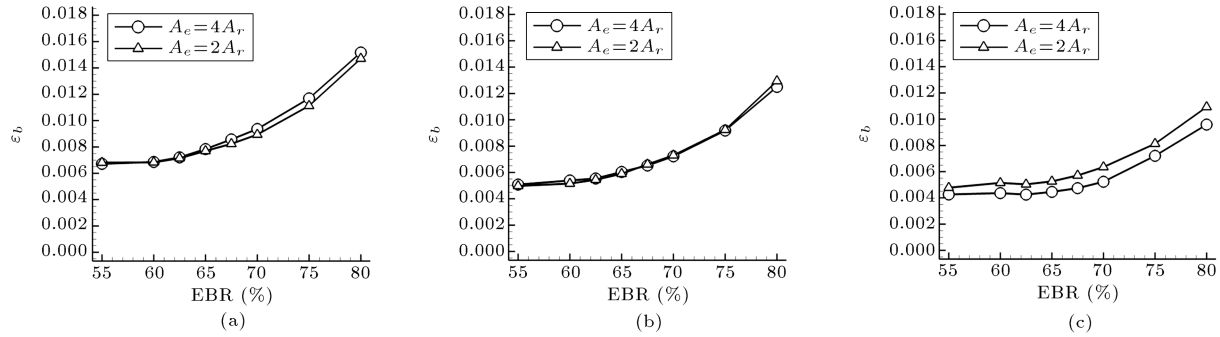

Figure 10. Variation of the bleed mass flow ratio for two bleed exit areas: (a) $M_\infty = 1.8$, (b) $M_\infty = 2.0$, (c) $M_\infty = 2.2$.

the freestream Mach number and bleed exit area on the stability margin, frequency, and amplitude of the buzz oscillations were studied. Results showed that stability margin of the intake for both configurations with and without bleed decreased when the freestream Mach number increased. In the bleed-off configuration case, the stability margin decreased by about 12% as the freestream Mach number increased from 1.8 to 2.2. In addition, in this configuration, the frequency of oscillations increased when the freestream Mach number decreased or when back pressure increased. Boundary layer suction was seen to considerably improve the intake stability margin. At $M_\infty = 1.8$, the intake was completely stable for all EBRs examined in this research. In contrast, in the bleed-off configuration, when the bleed was applied, as the freestream Mach number increased, frequency of the buzz increased and the spatial domain of the shock oscillations was limited to a small distance downstream of the bleed entrance. Three different frequency bands, namely about 100 Hz and 475 Hz for the bleed-off configuration and 900 Hz for the configuration equipped with bleed, were observed in this study. The differences were due to the buzz triggering mechanism that moved from Dailey criterion to Ferri criterion when the boundary layer suction was applied. It was seen that the exit area of the bleed duct did not have significant effects on the stability characteristics of the intake.

Acknowledgment

This study was financially supported by Ferdowsi University of Mashhad (FUM), Iran (Grant No. 41211).

Nomenclature

A	Area, m^2
CR	Contraction ratio
d	Maximum diameter of the intake, m
$Freq.$	Frequency, Hz
l	Model characteristic length, m
M	Mach number
$\dot{m}$	Mass flow rate, kg/s
MR	Main rake
P	Static pressure, Pa
PR	Single-probe rake
R	Gas constant, J/(kgK)
SM	Stability margin, %
T	Static temperature, K
TR	Throat rake
x	Axial coordinate, m
γ	Ratio of specific heat coefficients
ε	Mass flow ratio
η	Total pressure recovery, %

Subscripts

b	Bleed
e	Exit of the bleed duct
i	Inlet of the model
r	Reference area of the bleed
t	Total or stagnation quantity
∞	Freestream

References

1. Seddon, J. and Goldsmith, E.L., *Intake Aerodynamics*, pp. 268–284, Collins, London, UK (1985).
2. Oswatitsch, K., *Pressure Recovery in Missile in Reaction Propulsion at High Supersonic Speeds*, NACA TM 1140 (1947).
3. Soltani, M.R. and Sepahi-Younsi, J. "Buzz cycle description in an axisymmetric mixed-compression air intake", *AIAA Journal*, **54**, pp. 1040–1053 (2016).
4. Hill, P.G. and Peterson, C.R., *Mechanics and Thermodynamics of Propulsion*, 2nd Edn., pp. 217–273, Addison-Wesley, New York, US (1992).
5. Hankey, W.L. and Shang, S.J., *Analysis of Self-Excited Oscillations in Fluid Flows*, AIAA Paper 1980–1346 (1980).
6. Ferri, A. and Nucci, L.M., *The Origin of Aerodynamic Instability of Supersonic Inlet at Subcritical Condition*, NACA RM L50K30 (1951).

7. Dailey, C.L. "Supersonic diffuser instability", Ph.D. Dissertation, California Inst. of Technology, Pasadena, CA (1954).
8. Fisher, S.A., Neale, M.C., and Brooks, A.J. "On the subcritical stability of variable ramp intakes at Mach number around 2.0", National Gas Turbine Establishment Rept. ARC-R/M-3711 (1970).
9. Trapier, S., Duveau, P., and Deck, S. "Experimental study of supersonic inlet buzz", *AIAA Journal*, **44**, pp. 2354–2365 (2006).
10. Newsome, R.W. "Numerical simulation of near-critical and unsteady, subcritical inlet flow", *AIAA Journal*, **22**, pp. 1375–1379 (1984).
11. Sterbentz, W.H. and Davids, J., *Amplitude of Supersonic Diffuser Flow Pulsations*, NACA RM E52I24 (1952).
12. Sterbentz, W.H. and Evvard, J.C., *Criterions for Prediction and Control of Ram-jet Flow Pulsations*, NACA TN 3506 (1955).
13. Trimpi, R.L. "A Theory for stability and buzz pulsation amplitude in ram jets and an experimental investigation including scale effects", NACA Rept. 1265 (1956).
14. Nagashima, T., Obokata, T., and Asanuma, T. "Experiment of supersonic air intake buzz", Institute of Space and Aeronautical Science Rept. 481; also Institute of Space and Astronautical Science Report 37, **7**, pp. 165–209 (1972).
15. Bogar, T.J., Sajben, M., and Kroutil, J.C. "Characteristic frequencies in transonic diffuser flow oscillations", *AIAA Journal*, **21**, pp. 1232–1240 (1983).
16. Park, I., Ananthkrishnan, N., and Tahk, M. "Low-order model for buzz oscillations in the intake of a ramjet engine", *Journal of Propulsion and Power*, **27**, pp. 503–506 (2011).
17. Shi, X., Chang, J.T., and Bao, W. "Supersonic inlet buzz margin control of ducted rockets", *Proc. IMechE, Part G: J. Aerospace Engineering*, **224**, pp. 1131–1139 (2011).
18. Lu, P. and Jain, L. "Numerical investigation of inlet buzz flow", *Journal of Propulsion and Power*, **14**, pp. 90–100 (1998).
19. Trapier, S., Deck, S., and Duveau, P. "Delayed detached-eddy simulation and analysis of supersonic inlet buzz", *AIAA Journal*, **46**, pp. 118–131 (2008).
20. Namkoung, H.J., Hong, W.R, and Kim, J.M. "Effects of angles of attack and throttling conditions on supersonic inlet buzz", *Int'l J. of Aeronautical & Space Sci.*, **13**, pp. 296–306 (2012).
21. Fujiwara, H., Murakami, A., and Watanabe, Y., *Numerical Analysis on Shock Oscillation of Two-dimensional External Compression Intakes*, AIAA Paper 2002-2740 (2002).
22. Vivek, P. and Mittal, S. "Buzz instability in a mixed-compression air intake", *Journal of Propulsion and Power*, **25**, pp. 819–822 (2009).
23. Yeom, H.W., Kim, S.J., and Sung, H.G., *Inlet Buzz and Combustion Oscillation in an Axisymmetric Ramjet Engine*, AIAA Paper 2010-756 (2010).
24. Lee, H.J., Lee, B.J., and Kim, S.D. "Flow characteristics of small-sized supersonic inlets", *Journal of Propulsion and Power*, **27**, pp. 306–318 (2011).
25. Kwak, E. and Lee, S., *Convergence Study of Inlet Buzz Frequency with Computational Parameters*, AIAA Paper 2011-3362 (2011).
26. Nakayama, T., Sato, T., and Akatsuka, M., *Investigation on Shock Oscillation Phenomenon in a Supersonic Air Inlet*, AIAA Paper 2011-3094 (2011).
27. Hong, W. and Kim, C., *Numerical Study on Supersonic Inlet Buzz under Various Throttling Conditions and Fluid-Structure Interaction*, AIAA Paper 2011-3967 (2011).
28. Chima, R.V., *Analysis of Buzz in a Supersonic Inlet*, NASA/TM-2012-217612 (2012).
29. Kim, S.J., Yeom, H.W., and Sung, H.G., *Inlet Buzz and Combustion Oscillation in a Liquid-Fueled Ramjet Engine*, AIAA Paper 2011-230 (2011).
30. Nishizawa, U., Kameda, M., and Watanabe, Y., *Computational Simulation of Shock Oscillation around a Supersonic Air-Intake*, AIAA Paper 2006-3042 (2006).
31. Kotteda, V.M.K. and Mittal, S. "Viscous flow in a mixed compression intake", *Int. J. Numer. Meth. Fluids*, **67**, pp. 1393–1417 (2011).
32. Kotteda, V.M.K. and Mittal, S. "Finite element computation of buzz instability in supersonic air intakes", *A Chapter in Advances in Computational Fluid-Structure Interaction and Flow Simulation*, Springer, pp. 65–76 (2016).
33. Herges, T.G., Dutton, J.C., and Elliott, G.S., *High-Speed Schlieren Analysis of Buzz in a Relaxed-Compression Supersonic Inlet*, AIAA Paper 2012-4146 (2012).
34. Tindell, R.H. "Inlet drag and stability considerations for $M_0 = 2.00$ design", *J. Aircraft*, **18**, pp. 943–950 (1981)
35. Hongprapas, S., Kozak, J.D., and Moses, B., *A Small Scale Experiment for Investigating the Stability of a Supersonic Inlet*, AIAA Paper 97-0611 (1997).
36. Tan, H., Sun, S., and Yin, Z. "Oscillatory flows of rectangular hypersonic inlet unstart caused by downstream mass-flow choking", *Journal of Propulsion and Power*, **25**, pp. 138–147 (2009).
37. Chang, J., Wang, L., and Bao, W. "Novel oscillatory patterns of hypersonic inlet buzz", *Journal of Propulsion and Power*, **28**, pp. 1214–1221 (2012).
38. Trapier, S., Deck, S., and Duveau, P. "Time-frequency analysis and detection of supersonic inlet buzz", *AIAA Journal*, **45**, pp. 2273–2284 (2007).
39. Herrmann, D. and Triesch, K. "Experimental investigation of isolated inlets for high agile missiles", *Aerospace Science and Technology*, **10**, pp. 659–667 (2006).

40. Hirschen, C., Herrmann, D., and Gülhan, A. "Experimental investigations of the performance and unsteady behaviour of a supersonic intake", *Journal of Propulsion and Power*, **23**, pp. 566–574 (2007).

41. Herrmann, D., Triesch, K., and Gülhan, A. "Experimental study of chin intakes for airbreathing missiles with high agility", *Journal of Propulsion and Power*, **24**, pp. 236–244 (2008).

42. Herrmann, D., Blem, S., and Gülhan, A. "Experimental study of boundary-layer bleed impact on ramjet inlet performance", *Journal of Propulsion and Power*, **27**, pp. 1186–1195 (2011).

43. Herrmann, D., Siebe, F., and Gülhan, A. "Pressure fluctuations (buzzing) and inlet performance of an airbreathing missile", *Journal of Propulsion and Power*, **29**, pp. 839–848 (2013).

44. Herrmann, D. and Gulhan, A. "Experimental analyses of inlet characteristics of an airbreathing missile with boundary-layer bleed", *Journal of Propulsion and Power*, **31**, pp. 170–179 (2015).

45. Soltani, M.R., Farahani, M., and Asgari Kaji, M.H. "An experimental study of buzz instability in an axisymmetric supersonic inlet", *Scientia Iranica*, **18**, pp. 241–249 (2011).

46. Soltani, M.R. and Farahani, M. "Experimental investigation of effects of Mach number on the flow instability in a supersonic inlet", *Experimental Techniques*, **37**, pp. 46–54 (2013).

47. Soltani, M.R. and Farahani, M. "Effects of angle of attack on the inlet buzz", *Journal of Propulsion and Power*, **28**, pp. 747–757 (2012).

48. Soltani, M.R., Sepahi-Younsi, J., and Farahani, M. "Effects of boundary-layer bleed parameters on supersonic intake performance", *Journal of Propulsion and Power*, **31**, pp. 826–836 (2015).

49. Soltani, M.R., Daliri, A., and Sepahi-Younsi, J. "Effects of bleed position on the stability of a supersonic inlet", *Journal of Propulsion and Power*, **32**, pp. 1153–1166 (2016).

50. Kowalski, K. and Piercy, T.G., *Stability of Supersonic Inlets at Mach 1.91 with Air Injection and Suction*, NACA RM E56D12 (1956).

51. Griggs, C.F., *An Investigation of Two Methods of Suppressing Shock Oscillation Ahead of Conical Centre-Body Intakes*, Aeronautical Research Council, C.P. No. 605 (1962).

52. Trimpi, R.L. and Cohen, N.B., *Effect of Several Modifications to Center Body and Cowling on Subcritical Performance of a Supersonic Inlet at Mach number of 2.02*, NACA L55C16 (1955).

53. Obery, L.J. and Cubbison, R.W., *Effectiveness of Boundary Layer Removal Near Throat of Ramp Type Side Inlet at Free Stream Mach Number of 2.0*, NACA RM E54I14 (1954).

54. Obery, L.J., Englert, G.W., and Nussdorfer, T.J., *Pressure Recovery, Drag, and Subcritical Stability Characteristics of Conical Supersonic Diffusers with Boundary Layer Removal*, NACA RM E51H29 (1952).

55. Soltani, M.R., Sepahi-Younsi, J., and Daliri, A. "Performance investigation of a supersonic air intake in the presence of the boundary layer suction", *Proc. IMechE Part G: J. Aerospace Engineering*, **229**, pp. 1495–1509 (2014).

56. Mattingly, J.D. "Elements of propulsion: gas turbines and rockets", *AIAA Education Series*, Blacksburg, Chapter 8 (2006).

57. Soltani, M.R., Abedi, M., and Sepahi-Younsi, J. "Experimental investigation of the buzz cycle in a supersonic axisymmetric intake", *Modares Mechanical Engineering*, **14**, pp. 311–320 (2015) (in Persian).

Biographies

Javad Sepahi-Younsi was born in 1985 in Younsi, Gonabad, Iran. He received his MS and PhD degrees in Propulsion from the Aerospace Engineering Department at Sharif University of Technology, Tehran, Iran. He is now an Assistant Professor in the Mechanical and Aerospace Engineering Department at Ferdowsi University of Mashhad, Mashhad, Iran. He works in the field of numerical and experimental aerodynamics.

Mohammad Reza Soltani received his PhD degree in Aerodynamics from the University of Illinois at Urbana-Champaign, USA, and is now a Professor in the Aerospace Engineering Department at Sharif University of Technology, Tehran. His research interests include applied aerodynamics, unsteady aerodynamics, wind tunnel testing, wind tunnel design, and data processing.

Mahdi Abedi received his BS degree in Aerospace Engineering from Amirkabir University of Technology, Tehran, Iran, and his MS in Aerodynamics from the Aerospace Engineering Department at Sharif University of Technology, Tehran, Iran. His field of interest is experimental aerodynamics.

Mehran Masdari received his MS and PhD degrees in Aerodynamics from the Aerospace Engineering Department at Sharif University of Technology, Tehran, Iran. He is now an Assistant Professor in the Aerospace Engineering Department of the Faculty of New Sciences and Technologies, Tehran, Iran. He works in the field of experimental aerodynamics.